CHALMERS
UNIVERSITY OF TECHNOLOGY

Wideband Cartesian RF-DAC-Based Predistorter using Nonlinear RF-DACs and IQ Expansion

Wideband Cartesian RF-DAC-Based Predistorter using Nonlinear RF-DACs and IQ Expansion

Victor Åberg*, Han Zhou†
Email: victor.aberg@eit.lth.se, han.zhou@chalmers.se
*Lund University, Lund, Sweden
†Chalmers University of Technology, Gothenburg, Sweden

***Abstract*—We here present an RF-DAC-based PD featuring IQ expansion, a linearization concept using segmented non-linear RF-DACs combined with increased expansion in the IQ direction. The proposed predistorter, realized within the RF-DACs themselves, is very hardware efficient, only requiring a small amount of additional hardware compared to a conventional RF-DAC. The proposed RF-DAC-based PD, realized in a 22 nm CMOS technology, is used to linearize a PA integrated on the same chip. With IQ expansion, we measure a peak compression ripple of ±0.2 dB across the full range with a peak output power <2.3 dB below the PA P_{sat}. Modulated measurements with up to 4 GSym/s 64QAM SC signals show an EVM <4.05 % and ACPR <−30.1 dBc, achieving an EVM improvement of >0.3 percent unit.**

***Index Terms*—CMOS, PA, RF-DAC-based predistorter, RF-IQ modulator, Wideband**

I. Introduction

Modern cmWave and mmWave communication systems combine spectrum-efficient modulation formats and >1 GHz continuous spectrum with massive multiple-input-multiple-output (mMIMO) arrays [1], [2]. To further improve capacity, frequency resources from multiple bands may be combined through stitching, stressing the need for wideband transmitters. With large numbers of densely packed transmitters and antennas, strict area, energy, and thermal budgets will follow [3]. Thus, highly linear, energy efficient, and wideband transmitters are essential, while the antenna gain brought by the mMIMO array relaxes the per-element output power requirement.

RF-DACs are a suitable candidate for these wideband transmitters, combining digital-to-analog (D/A) conversion with up-conversion in a single block, allowing for wideband signals to be generated close to the antennas [4], [5]. However, in mMIMO arrays, having a RF-IQ modulator per antenna element may be infeasible, rather, a single RF-IQ modulator may drive several PAs, realizing a hybrid beamforming block.

The inverse relationship between PA compression level and linearity is well known. To fulfill linearity requirements, the PA is either operated at significant back-off, or a predistorter (PD) is required to compensate for the non-linear characteristic. Digital predistortion (DPD) has been the go-to solution for improving linearity for quite some time. However, in wideband systems, even simple realizations are costly as computations are performed on every sample [3], [6]. The power consumption for realizing DPD may approach or even exceed that of the PA in a large MIMO array, making alternative approaches desirable.

This research has in part been carried out in classIC, a joint venture between Chalmers University of Technology, Lund University, Acconeer, Axis Communications, Cadence Design Systems, Codasip, Ericsson, Frontgrade Gaisler, GlobalFoundries, Qamcom, and Saab, financed by the Swedish Foundation for Strategic Research (SSF). This research was in part supported by Sweden's Innovation Agency (VINNOVA), Sivers Semiconductors, and Chalmers University of Technology under Grant 2022-00863.

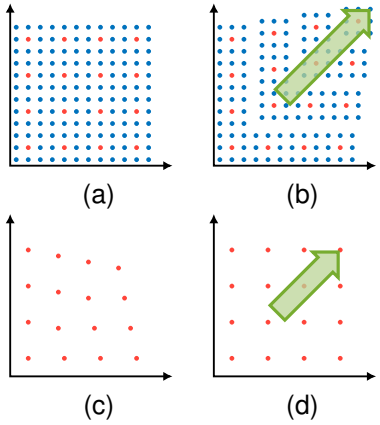

Fig. 1. Cartesian modulator output amplitude/phase combinations for single quadrant using (a) conventional modulator (b) modulator with IQ expansion. (c) and (d) Resulting partial constellation at the PA output when using each respective modulator. These points represents the red points in (a) and (b).

The Cartesian RF-DAC-based predistorter (PD) was introduced to efficiently realize predistortion of wideband signals, with a cost only marginally higher than that of a conventional Cartesian RF-IQ modulator [7]. The predistortion is realized using non-linear RF-DACs with an expanding characteristic. In a Cartesian modulator, these provide independent 1D linearization of the in-phase (I) and quadrature-phase (Q) components. Excellent linearization performance is achieved in the I/Q directions, but degraded in the IQ direction. To further improve linearity, we here introduce RF-DAC-based PD with IQ expansion, boosting the expanding characteristic in the IQ direction without degrading the capabilities in the I/Q directions.

II. IQ Expansion

The Cartesian RF-DAC-based PD suffers from poor linearization performance when both RF-DACs are active,

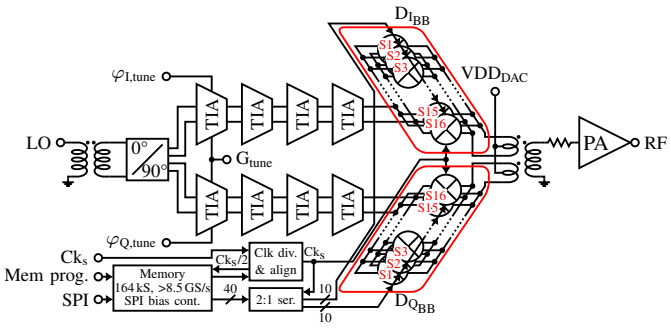

Fig. 2. Transmitter block diagram showing the realization of the complete RF path. RF-DACs are encircled in red.

see partial constellation at the PA output in Fig. 1c. We here introduce IQ expansion, a more aggressive expanding characteristic in the IQ direction, improving the linearity in the IQ direction without degrading the linearity in the I/Q directions. The amplitude/phase combinations in a single quadrant are shown for a conventional Cartesian RF-IQ modulator in Fig. 1a and with IQ expansion applied in Fig. 1b. It can here be observed that IQ expansion will shift points outwards in the 45° direction. This expansion is achieved by activating additional unit cells at equidistant steps upto min(I,Q); note the increased step size in Fig. 1b. In addition to maximizing the expansion in the 45° direction, this approach also realize a gradual transition in additional expansion; no further expansion is added in the I/Q directions while maximum expansion is introduced in the IQ direction. This well matches the characteristics of the PA compression when mapped through the modulator to the digital input codes. The constellation points at the PA output are shown with and without expansion in Fig. 1d and Fig. 1c respectively, assuming uniform RF-DACs; the implementation presented below uses segmented non-linear RF-DACs to realize linearization capabilities also in the I/Q direction.

Two expanding profiles now need to be selected. First, the expanding scaling is chosen for a single RF-DAC to achieve good linearity in the I/Q directions. The IQ expansion is then selected for the direction requiring the most additional expansion, that is, when equal codes are provided to both RF-DACs. Only a limited amount of IQ expansion is required for low IQ codes, while significant IQ expansion is needed for high IQ codes.

III. Design

A block diagram for the complete transmitter is shown in Fig. 2, including the RF-DAC-based PD, the PA being linearized, and the waveform memory used to provide test sequences. The PA uses a topology based on a neutralized stacked differential pair. The RF-DACs are capable of delivering a higher output power than the PA requires. To align the power levels, a 5 dB attenuator is placed between the RF-DACs and the PA; the RF-DACs are capable of driving more than a single PA, envision the hybrid beamforming block.

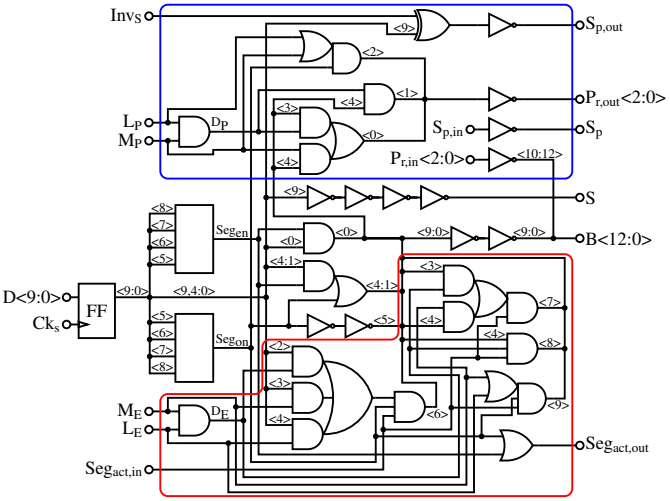

Fig. 3. Schematic of the segment control logic. Gates encircled in red control IQ expansion and gates encircled in blue control phase compensation.

Accurate quadrature LO signals are essential for a Cartesian modulator outputting higher-order QAM signals. Additionally, to tune the expanding characteristic, a tunable LO magnitude is required. The LO generation is further complicated by the large capacitive load presented by the RF-DACs (a large total transistor width combined with the distribution of the LO signals to all unit cells). The quadrature LO signals are generated and buffered using a current-mode logic (CML) divider followed by four-stage trans-impedance amplifiers (TIAs), separated by differential series inductors and series capacitors. The first TIA has a tunable gain.

The two 10-bit segmented RF-DACs with expanding characteristic that form the Cartesian RF-DAC-based PD are encircled in red in Fig. 2. These RF-DACs are divided into 16 segments, each having a unique scale factor. The number of segments is a trade-off between the ability to approximate the expanding characteristic and the complexity of the control logic. Additionally, a fast and minimalistic segment control logic is vital for efficient operation at high sample rates. A schematic for the segment control logic is shown in Fig. 3. The logic is identical in all segments, except for the two gates

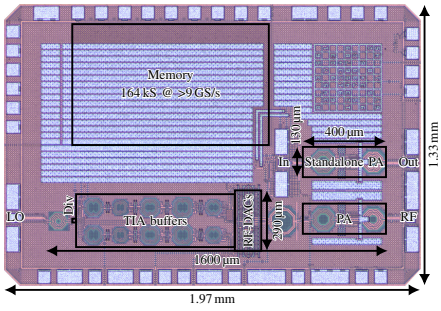

Fig. 4. Chip photo showing the complete transmitter, the standalone PA and the waveform memory.

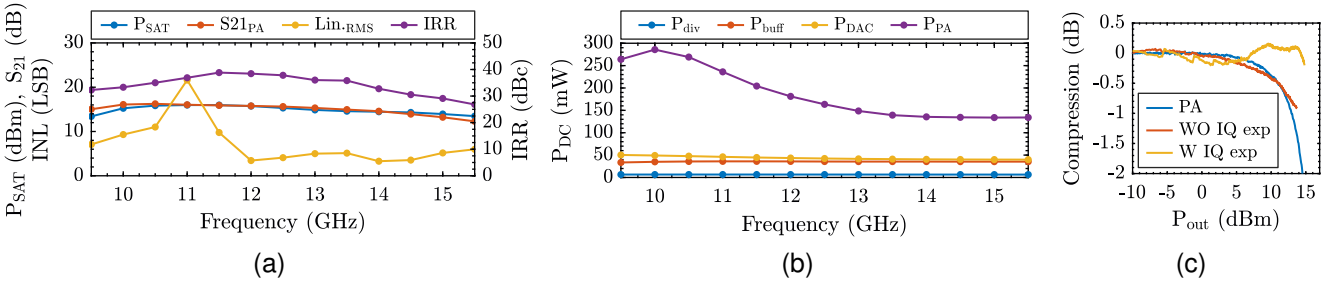

Fig. 5. (a) Saturated RF output power, PA small-signal gain, image-rejection ratio, and integral non-linearity versus carrier frequency. (b) DC power consumption for the divider, TIA buffers, RF-DACs (excluding digital circuits), and PA versus carrier frequency. (c) Compression versus output power for the standalone PA (including attenuator), and for the transmitter with and without IQ expansion enabled. RF-DACs are simultaneously fed with identical input codes.

realizing Seg_{en} and Seg_{on}, these are unique to each segment. The former activates the segment while the latter activates all unit cells in a segment. The additional logic required for enabling IQ expansion is encircled in red. Logic used to control AM/PM compensation is encircled in blue.

The IQ expansion should ideally be realized such that 1 LSB is activated every 4th, 8th, or 16th code upto the minimum I/Q code, however, very complex logic would result. For a substantially reduced logic complexity, activation of IQ expansion cells is realized on a per segment basis, using Seg_{en}+Seg_{on}, with a marginal reduction in the resulting linearization performance. The code-stepping is configured using the L_E and M_E signals. The AM/PM compensation activates 1 LSB cell in the corresponding segment in the other RF-DAC, every 8th, 16th, or 32nd code, configured by the L_P and M_P signals; the sign is set by Inv_S. The control signals for both the IQ expansion and the AM/PM compensation may be independently configured for each segment, potentially at the cost of reduced capabilities at the highest codes.

The impedance matching for both divider and PA is realized using interleaved baluns implemented in the top-most copper metal layers. This is also the case for the differential series inductors and the custom balun with dual primary coils that is used to enhance isolation between the RF-DAC outputs, reducing cross-modulation distortion.

A 164 kS >9 GS/s SRAM waveform memory provide baseband I/Q signals to the transmitter. On-chip digitally programmable bias sources are used to reduce pad count.

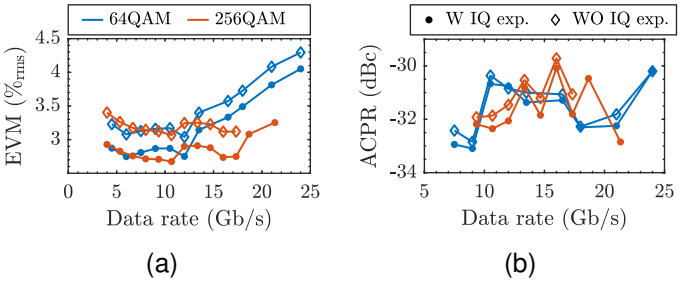

Fig. 6. (a) EVM and (b) ACPR across data rate for 64QAM and 256-QAM SC signals.

IV. Experimental Results

A chip photo of the full transmitter using the proposed PD, the waveform memory, and the standalone PA is shown in Fig. 4. The chip has been fabricated using GlobalFoundries 22FDX and the design measures 1.97 mm × 1.33 mm; the transmitter occupies 1600 µm × 290 µm.

All measurements, using both continuous-wave (CW) and wideband modulated signals, were performed using a Keysight PNA-X vector network analyzer.

A. Continuous-wave measurements

The static performance, that is, the peak output power (P_{sat}), image-rejection ratio (IRR), integral non-linearity (INL), and PA small-signal gain are presented in Fig. 5. The peak output power at 11 GHz is 16 dBm and 15.4 dBm with and without IQ expansion enabled. The 3 dB CW bandwidth is 9.5–15.75 GHz for the complete transmitter and 9–15 GHz for the standalone PA. An IRR >35 dBc is achieved between 10.25–13.5 GHz and the INL for a single RF-DAC is <6 LSB between 12–16.5 GHz, using a fixed bias setting. The DC power consumption for the

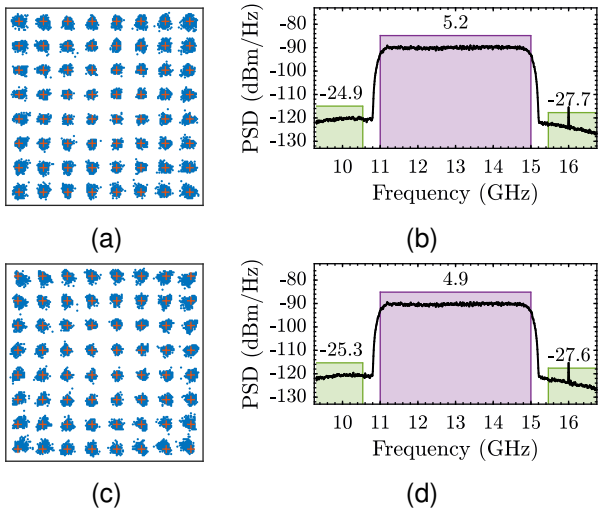

Fig. 7. Constellation diagram and output spectra for 64QAM SC signals using IQ expansion (a) and (b), EVM 4.05 % and ACPR −30.1 dBc, and without using IQ expansion (c) and (d), EVM 4.29 % and ACPR −30.2 dBc. Both use a sample rate of 8 GS/s, achieving a data rate of 24 Gb/s with a BER $<10^{-4}$. Channel power reported in dBm.

TABLE I
PERFORMANCE COMPARISON AGAINST OTHER STATE-OF-THE-ART RF-DAC-BASED TRANSMITTERS SUPPORTING AT-LEAST 64QAM.

	This work			[4]	[5]	[7]	[8]	[9]
	W. IQ exp.		Wo. IQ exp.					
Technology	22 nm SOI			45 nm SOI	28 nm	22 nm SOI	45 nm	22 nm SOI
Topology	Cartesian (expanding) + PA			Cartesian	Cartesian	Cartesian (exp.) + PA	Cartesian	Cartesian
Resolution [b]	2×10			2×6	2×10	2×10	2×8	2×6
Frequency [GHz]	9.5–15.75			18–32	20–32	10–13.5	21–31	28–30
Peak P_{SAT} [dBm]	16.0		15.4	19.9	19.02	15.8	1.5	21.2
Modulation format	64QAM SC	256QAM SC	64QAM SC	64QAM SC	64QAM SC	64QAM SC	64QAM SC	64QAM SC
Sample rate [GS/s]	8	8	8	2[1]	2	7	2.25	2.4
OSR	2	3	2	1	4	2	4	-
EVM [$\%_{rms}$]	4.05[2]	3.25[2]	4.29[2]	4	3.59	3.83	2.18	3.32
ACPR [dBc]	−30.1[2,3]	−32.8[2,3]	−30.2[2,3]	-	−33.6	−32.4[3]	−33.75	−30.8
Data rate [Gb/s]	24	21.3	24	12	3	21	2.25	2.4
Peak energy eff. [pJ/b]	12.23	13.6	12.20	75[4]	48.7[4]	12.4	56	68
Area [mm^2]	<0.47			2.41[5]	0.2	<0.47	0.3	2.2[5]

[1] Highest sample rate achieving at least 64QAM. [2] Settings identical, except for IQ expansion
[3] Computed for 400 MHz and scaled to signal bandwidth. [4] Estimated based on data in paper. [5] Including pads.

divider, TIA buffers, RF-DACs (excluding the digital circuits), and PA is shown across frequency in Fig. 5b.

The compression is plotted versus output power for the standalone PA, and for the transmitter with and without IQ expansion enabled while providing the same input code to both RF-DACs. With IQ expansion enabled, the ripple in the compression is limited to ±0.2 dB while achieving a P_{sat} for the transmitter <2.3 dB below the P_{sat} for the standalone PA.

B. Wideband modulated measurements

The performance, using wideband 64QAM and 256QAM single-carrier (SC) signals, centered at 13 GHz, are here evaluated both with and without IQ expansion. The 64-QAM signals are up-sampled 2x through an RRC filter while 3x up-sampling is used for 256QAM. The input signals are scaled in the digital domain to maximize dynamic range without clipping the signal. In Fig. 6, EVM and ACPR are plotted versus data rate for both modulation formats, with and without IQ expansion. The constellation diagrams and output spectra for 64QAM SC signals in Fig. 7 demonstrates the benefit with IQ expansion. The compression seen in Fig. 7c is removed in Fig. 7a when IQ expansion is enabled. This is also visible for the 256QAM signals in Fig. 8. The ACPR is calculated using the noise power in an adjacent 400 MHz channel scaled to the channel bandwidth. This is done to overcome limitations in the measurement setup; actual ACPR is likely better.

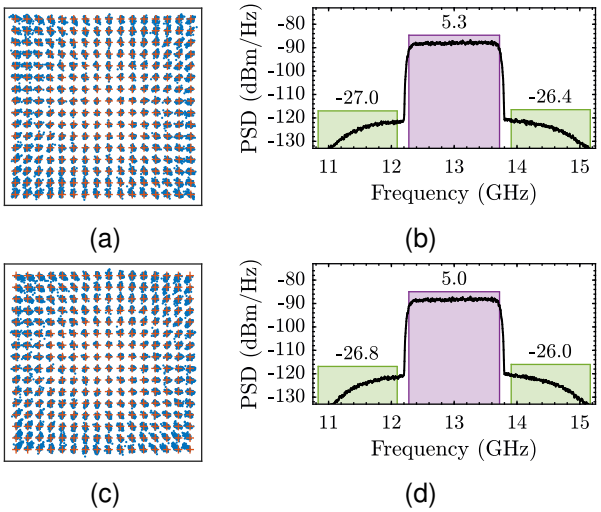

Fig. 8. Constellation diagram and output spectra for 256QAM SC signals using IQ expansion (a) and (b), EVM 2.75 % and ACPR −31.8 dBc, and without using IQ expansion (c) and (d), EVM 3.12 % and ACPR −31 dBc. Both use a sample rate of 6.5 GS/s, achieving a data rate of 17.3 Gb/s with a BER $<10^{-3}$. Channel power reported in dBm.

With modulated signals at 8 GS/s, the PA consumes 135.5 mW and the RF-DACs 8.6 mW for the analog parts and 106.7 mW for the logic. The power consumption for the divider and TIA buffers is the same as in the CW case.

Table I summarizes the performance for the RF-DAC-based PD and compares it with other state-of-the-art RF-DAC-based transmitters. With IQ expansion, EVM is improved by >0.3 percent unit and the average channel power is increased by 0.3 dB when IQ expansion is used.

V. CONCLUSION

We here introduce IQ expansion, an approach to improve the lineairzation capabilities for a Cartesian RF-DAC-based PD. With IQ expansion, a peak ripple in the compression of ±0.2 dB is achieved with an output power <2.3 dB below the PA P_{sat}. The EVM is improved by 0.3 % and channel power by 0.3 dB using IQ expansion for spectral-efficient SC signals.

ACKNOWLEDGEMENT

We thank GlobalFoundries for the chip fabrication, Keysight for the PNA-X software, and the Kollberg laboratory for instrument access.

REFERENCES

[1] *Base Station (BS) radio transmission and reception*, 3GGP Std. 38.104, Sep. 2021.

[2] E. Semaan, E. Tejedor, R. K. Kochhar, S. Magnusson, and S. Parkvall, "6G spectrum - enabling the future mobile life beyond 2030," White Paper, Feb 2023. [Online]. Available: https://www.ericsson.com/en/reports-and-papers/white-papers/6g-spectrum-enabling-the-future-mobile-life-beyond-2030

[3] H. Huang, J. Xia, and S. Boumaiza, "Novel parallel-processing-based hardware implementation of baseband digital predistorters for linearizing wideband 5G transmitters," *IEEE Transactions on Microwave Theory and Techniques*, vol. 68, no. 9, pp. 4066–4076, 2020.

[4] S. Shopov, N. Cahoon, and S. P. Voinigescu, "Ultra-broadband I/Q RF-DAC transmitters," *IEEE Transactions on Microwave Theory and Techniques*, vol. 65, no. 12, pp. 5411–5421, Dec 2017.

[5] H. J. Qian, Y. Shu, J. Zhou, and X. Luo, "A 20-32-GHz quadrature digital transmitter using synthesized impedance variation compensation," *IEEE Journal of Solid-State Circuits*, vol. 55, no. 5, pp. 1297–1309, 2020.

[6] A. Katz, J. Wood, and D. Chokola, "The evolution of PA linearization: From classic feedforward and feedback through analog and digital predistortion," *IEEE Microwave Magazine*, vol. 17, no. 2, pp. 32–40, 2016.

[7] V. Åberg, P. Saad, R. Hou, and H. Zhou, "RF-DAC-based PA pre-distortion using expanding non-linear RF-DAC scaling," in *19th European Microwave Integrated Circuits Conference (EuMIC)*, 2024, pp. 267–270.

[8] H. J. Qian, W. Qin, C. Qiu, and Y. Yang, "A 21-to-31 GHz DPD-less quadrature RFDAC with invariant impedance and scalable LO leakage," in *IEEE International Solid-State Circuits Conference (ISSCC)*, vol. 68, 2025, pp. 106–108.

[9] H. M. Nguyen, J. S. Walling, A. Zhu, and R. B. Staszewski, "A mm-wave switched-capacitor RFDAC," *IEEE Journal of Solid-State Circuits*, vol. 57, no. 4, pp. 1224–1238, 2022.